Structure, Vol. 12, 2173–2183, December, 2004, ©2004 Elsevier Ltd. All rights reserved. DOI 10.1016/j.str.2004.09.012

Structural and Functional Properties of the Human Notch-1 Ligand Binding Region

Sophie Hambleton,[1,3,6] Najl V. Valeyev,[2,4] Andreas Muranyi,[2,4,5] Vroni Knott,[1] Jörn M. Werner,[1,7] Andrew J. McMichael,[3] Penny A. Handford,[1] and A. Kristina Downing[2,*]

[1]Division of Molecular and Cellular Biochemistry
[2]Division of Structural Biology
Department of Biochemistry
University of Oxford
South Parks Road
Oxford OX1 3QU
United Kingdom
[3]MRC Human Immunology Unit
The Weatherall Institute of Molecular Medicine
Headington
Oxford OX3 9DS
United Kingdom

Summary

We present NMR structural and dynamics analysis of the putative ligand binding region of human Notch-1, comprising EGF-like domains 11–13. Functional integrity of an unglycosylated, recombinant fragment was confirmed by calcium-dependent binding of tetrameric complexes to ligand-expressing cells. EGF modules 11 and 12 adopt a well-defined, rod-like orientation rigidified by calcium. The interdomain tilt is similar to that found in previously studied calcium binding EGF pairs, but the angle of twist is significantly different. This leads to an extended double-stranded β sheet structure, spanning the two EGF modules. Based on the conservation of residues involved in interdomain hydrophobic packing, we propose this arrangement to be prototypical of a distinct class of EGF linkages. On this premise, we have constructed a model of the 36 EGF modules of the Notch extracellular domain that enables predictions to be made about the general role of calcium binding to this region.

Introduction

The orderly development of complex multicellular organisms requires mechanisms for cell-cell coordination in the determination of cell fate. The Notch pathway fulfils this function in every metazoan species so far studied, in numerous tissues and during embryonic development and beyond (Lai, 2004). Null mutations of core components of the Notch pathway are lethal during embryonic development of laboratory animals, but a number of human diseases are being traced to more subtle derangements of Notch signaling (Harper et al., 2003).

Notch and its homologs (1–4 in mammals) are transmembrane proteins that function as receptors for ligands expressed on neighboring cell surfaces (named Delta and Serrate in *Drosophila*, Delta-like and Jagged in mammals). Signal transduction is remarkably direct; following ligand binding, the intracellular domain of Notch (N_{ICD}) is released by regulated intramembrane proteolysis at two sites and translocates to the nucleus, where it functions as a transcriptional regulator (Schweisguth, 2004). Recent work has identified a number of important regulators of the Notch pathway (reviewed in Schweisguth, 2004), but the interaction with ligand retains a crucial, permissive role.

A binding interaction between *Drosophila* Notch and ligand was first demonstrated in mixtures of singly transfected insect cells (Fehon et al., 1990). Later, deletion mutation analysis localized this binding activity to 2 of the 36 EGF-like repeats (EGFs) that constitute the majority of the Notch extracellular domain (Rebay et al., 1991). In developing *Drosophila*, deletion of this EGF pair (11 and 12) abrogates function and the ability to bind to Delta, although there is indirect evidence that some Serrate binding persists (Rebay et al., 1991; Lawrence et al., 2000). It is generally believed that Notch EGFs 11 and 12 interact with the conserved N-terminal "DSL" module of Notch ligands, together with adjacent regions including a variable number of EGFs (Han et al., 2000; Henderson et al., 1997; Shimizu et al., 1999).

Recent research has revealed that EGF12 within the ligand binding region contains an O-fucosylation site at Thr466 (Shao et al., 2003). Although O-fucosyl transferase activity is required for Notch function (Okajima and Irvine, 2002; Okajima et al., 2003), point mutagenesis of the EGF12 fucosylation site in *Drosophila* did not abrogate ligand binding or signaling activity (Lei et al., 2003). Instead, the unfucosylated mutant was rendered resistant to the action of Fringe, a glycosyl transferase that inhibits the interaction of Notch with Serrate/Jagged ligands (Lei et al., 2003; Moloney et al., 2000). Thus, fucosylation within the putative ligand binding region is not required for molecular recognition, but it appears to be critical to the appropriate regulation of Notch-ligand interaction by Fringe.

The EGF-like domain represents an evolutionarily conserved, modular structure that is found in a wide variety of proteins, often as arrays of multiple tandem repeats (Boswell et al., 2004). The secondary structure of individual domains is dominated by a core β-pleated sheet, three characteristic disulphide bonds, and a corresponding series of loops of variable composition. Notch EGFs 11–13 exemplify the calcium binding variety of EGF (cbEGF), based on amino acid sequence and on their behavior with chromophoric chelators (Rand et al., 1997). The ability to bind Ca^{2+} appears functionally im-

*Correspondence: kristy.downing@bioch.ox.ac.uk
[4]These authors contributed equally to this work.
[5]Present address: GE Healthcare, Chemical Characterisation, Protein Separations R&D, Amersham Biosciences AB, Björkgatan 30, SE-751 84 Uppsala, Sweden.
[6]Present address: Department of Pediatrics, Columbia University College of Physicians and Surgeons, Room BB431, 630 West 168th Street, New York, New York 10032.
[7]Present address: University of Southampton, School of Biological Sciences, Bassett Crescent East, Southampton, SO16 7PX, United Kingdom.

portant, based on the severe loss-of-function phenotype produced by a point mutation in a consensus Ca^{2+} binding residue in EGF12 (de Celis et al., 1993). In addition, it has recently been proposed that extracellular Ca^{2+} may regulate Notch signaling within a physiologically relevant concentration range (Raya et al., 2004).

Tandem repeats of cbEGFs have been identified in many different proteins, and mutations within them may be associated with human disease (Boswell et al., 2004). Multiple sequence alignment analysis has shown that in spite of the functional diversity of proteins containing tandem cbEGFs, the two domains are always linked by one or two amino acids, suggesting the existence of general pairwise domain architectures (Downing et al., 1996). For class I domains (separated by a single amino acid) such as fibrillin-1 and the low-density lipoprotein receptor, calcium is known to play an important structural role: it imparts rigidity to an extended tertiary structure (Cardy and Handford, 1998; Downing et al., 1996; Kielty and Shuttleworth, 1993; Saha et al., 2001; Smallridge et al., 2003; Werner et al., 2000) and protects against proteolytic degradation (McGettrick et al., 2000; Reinhardt et al., 2000). By analogy, one can envisage the involvement of Ca^{2+} in stabilizing a conformation of Notch that favors ligand binding and/or consequent signal transduction. However, the class II linkages between EGFs in Notch and its ligands (containing two amino acids) differ systematically from those of previously solved class I cbEGF domain pairs, with unknown structural implications.

In the current work, we take a step toward a molecular understanding of Notch-ligand interaction by characterizing the functional and structural properties of a recombinant fragment of human Notch-1 encompassing EGF domains 11–13. As anticipated, our results offer structural insight into the importance of calcium binding in Notch-ligand interactions. The structure also provides a prototypical example of the extended arrangement of tandem calcium-loaded cbEGF domains containing a two amino acid linker (Downing et al., 1996). Comparison of this structure with cbEGF domain pairs from fibrillin-1 and the LDL receptor suggests that the insertion of the extra amino acid plays an important role in determining the twist angle between the two domains, and hence modulates the surface presented for protein-protein interactions. Our work therefore provides a basis for protein engineering and site-directed mutagenesis experiments designed to probe the requirements for Notch-ligand binding.

Results

Previous work identified EGFs 11 and 12 as the minimal binding unit of *Drosophila* Notch (Rebay et al., 1991), and functional activity of this domain pair, expressed in bacteria, has been claimed (Garces et al., 1997; Nickoloff et al., 2002). However, in initial experiments, we were unable to achieve homogeneous in vitro refolding of hNotch-1 EGFs 11 and 12. We therefore produced the three-domain construct containing EGF domains 11–13 (N11–13), reasoning that the presence of the C-terminal EGF would stabilize the folding of EGF12, as has been

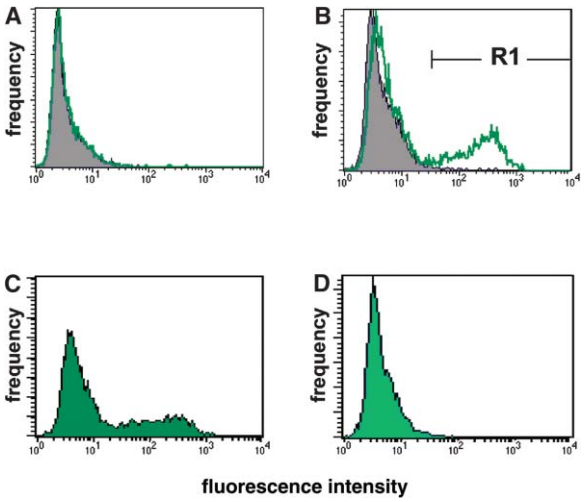

Figure 1. FACS Analysis of the Binding of Tetrameric Complexes of Recombinant Notch to the Surface of Ligand-Expressing Cells

(A and B) Intensity of surface staining with Notch cbEGF11–13-Extravidin-PE complexes (line) and unconjugated Extravidin-PE (fill). (A) Uninfected L cells. (B) L cells expressing murine Delta-like-1. The proportions of cells stained (region R1) were as follows (background staining in parentheses): uninfected L cells, 0.2% (0.1%); murine Delta-like-1, 24.0% (0.4%).

(C and D) Calcium dependence of Notch tetramer binding to murine Delta-1-expressing cells. (C) Surface staining in the presence of 1 mM calcium chloride. (D) Absence of staining upon substitution with 1 mM EGTA.

demonstrated for other EGF repeats (Kurniawan et al., 2004; Whiteman et al., 2001). In order to verify that this region could support ligand binding, a tagged version was engineered that, after refolding, could be specifically biotinylated for conjugation to a fluorescently labeled avidin derivative. Such technology has previously been applied very successfully to recombinant class I MHC molecules and their low-affinity interaction with cell surface TCR and CD8 ligands (Altman et al., 1996).

We used FACS to analyze binding of the resulting labeled tetrameric N11–13 complexes to L cells expressing Notch ligand at high levels following retroviral transduction. Control, uninfected L cells exhibited no tetramer staining (Figure 1A). In contrast, specific binding to cells expressing murine Delta-like 1 (K/D) was readily demonstrated (see Figure 1B). The intensity of staining (about two logs) was such that the tetramer-positive cells formed a discrete population comprising some 20% of cells (in keeping with transduction efficiency, data not shown). Removal of 1 mM ionized calcium from the staining buffer, and its replacement by EGTA, totally abrogated tetramer binding (compare Figures 1C and 1D). Thus, a requirement for Ca^{2+} is localized to this specific region of Notch and/or its binding partner. In contrast, preincubation with an excess of unconjugated N11–13 showed failure to compete with tetramer for binding to Notch ligand (data not shown), implying a low affinity for the monomeric interaction.

The structure of the N11–13 peptide without tag and in the presence of saturating calcium was solved on the basis of solution NMR data. A superposition of the family of structures is shown in Figure 2, and structural statis-

Figure 2. Superposition of the Family of NMR Structures

The 20 final structures of Notch cbEGF11–13, superposed on secondary structure backbone atoms of domains N11 and N12. The structure is oriented with the N terminus at the top. Secondary structure atoms that are highlighted in dark green correspond to the C^{α}, C', and N atoms of: N11: 415–418 (α); 427–431, 436–440, 444–445, 451–452 (β); N12: 455–458 (α); 466–470, 473–477, 482–483, 489–490 (β). The backbone rmsd to the mean for these atoms is 0.68 Å. Secondary structure residues for N13 are: 504–508, 511–515 (β). This figure and Figures 4, 5, and 7 were created with Molmol (Koradi et al., 1996).

Table 1. Summary of Structural Statistics

NOE upper distance limits	
Total	3,269
Intraresidue and sequential ($\|i - j\| = 1$)	2,466
Medium range ($1 < \|i - j\| < 5$)	368
Long range ($\|i - j\| \geq 5$)	417
Other NOE-type restraints	
H bonds	42
Calcium	15
Torsion angle restraints	
Total	87
ϕ	44
Ψ	43
Distance restraint violations	
Number><0.2Å>	5
Maximum	0.49 Å
Torsion angle restraint violations	
Number > 5°	none
CYANA target function	6.04 ± 0.35 Å^2

Convergence Parameters

	Cycle 1 Rmsd (Å)		Cycle 7 Rmsd (Å)	
	Backbone Atoms (C^α, C′, N)	Heavy Atoms	Backbone Atoms (C^α, C′, N)	Heavy Atoms
N11 (414–450)	0.96 ± 0.27	1.53 ± 0.31	0.53 ± 0.17	1.09 ± 0.21
N12 (451–488)	1.92 ± 0.57	2.60 ± 0.61	1.04 ± 0.37	1.58 ± 0.37
N13 (489–515)	2.74 ± 0.75	3.87 ± 1.05	1.21 ± 0.38	2.02 ± 0.42
N11–12 (414–488)	2.56 ± 0.84	3.04 ± 0.78	1.08 ± 0.31	1.54 ± 0.29
N11–13 (414–515)	5.65 ± 1.72	6.21 ± 1.69	—	—
N11 (414–450)	0.96 ± 0.27	1.53 ± 0.31.	0.53 ± 0.17	1.09 ± 0.21

PROCHECK	
Residues in favored regions (%)	61.5
Residues in additionally allowed regions (%)	27.5
Residues in generously allowed regions (%)	6.9

Results are shown as mean ± SD.

tics for the ensemble are given in Table 1. The first two domains comprising the Notch ligand binding region adopt a well-defined, elongated conformation. The NMR data for the third domain are highly line broadened, and consequently the structure of this domain and its relative orientation are less well defined. The accuracy of the NMR models may be assessed based on criteria, which have been defined by Jee and Güntert (Jee and Güntert, 2003), for successful structure calculation with the program CYANA. These criteria specify that in the final round of calculations, >75% of the input NOE cross peaks are assigned, and the backbone root mean square deviation (rmsd) of structures calculated in the first cycle must be <3 Å. The CYANA algorithm is composed of seven iterations in which structures calculated in the previous iteration are used as input for cycles 2–7. Therefore, convergence to a well-defined fold in the first iteration is critical to the accuracy of structure calculation with this program. Table 1 shows that the convergence criteria have been met for each of the three EGF domains in isolation, and for the N11–12 pair, but that the cycle 1 rmsd for all three domains is above the acceptable threshold. Therefore, the orientation of N13 with respect to N11–12 is not reliable in these models.

In order to gain insight into the true behavior of N13 with respect to N11–12, we acquired heteronuclear ^{15}N relaxation data at 11.7 and 14.1 T, which are shown in Figure 3. Plots of experimental T_1 and T_2 values versus curves calculated for T_1 and T_2 at different correlation times using the Lipari-Szabo formalism (Lipari and Szabo, 1989a) show that the dynamic behavior of N13 is distinctly different from N11–12. Points for N11 and N12 tend to cluster mainly in a single region of the plots shown in Figures 3A and 3B, indicating that there is little relative motion of the two domains and that they tumble with similar correlation times. Correlation times (±SEM) for the two domains calculated on the basis of the T_1 and T_2 data for residues with heteronuclear [^{1}H]-^{15}N NOE values higher than 0.65 are 8.6 ± 0.3 and 9.2 ± 0.2 ns at 11.7 T and 8.9 ± 0.3 and 9.4 ± 0.2 ns at 14.1 T, respectively. In contrast, the points for N13 show greater spread, with the majority of residues manifesting low T_2 values, which are indicative of slower timescale (μs–ms) chemical exchange. The T_2 values for this domain are consistent with the line broadening observed in the NOESY data. However, heteronuclear [^{1}H]-^{15}N NOE values for the construct, shown in Figure 3C, are relatively constant. Values less than 0.6 at 14.1 T are only associated with the N and C termini and loop regions, and not the interdomain linker regions. Analysis of the field dependence of the primary data clearly shows large R_{ex} contributions for a number of residues in N13. The data also indicate that the timescale of motions is outside the fast exchange approximation. Overall, these data

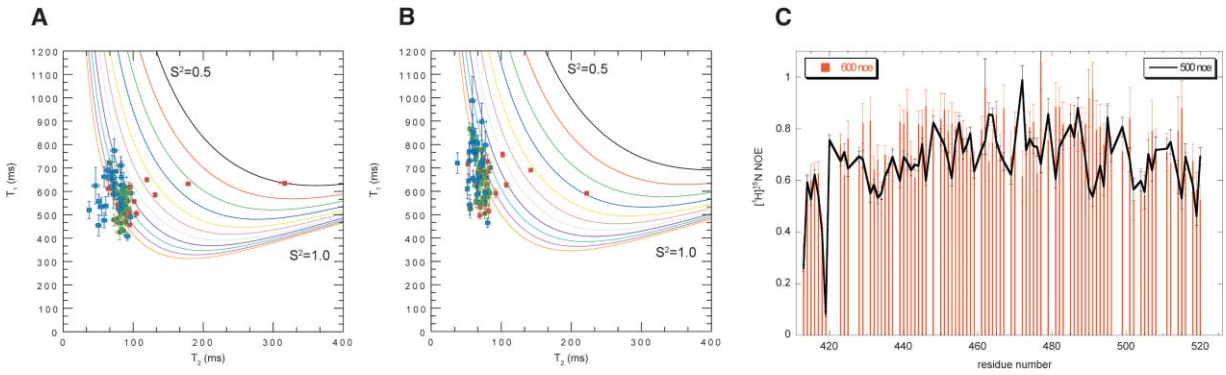

Figure 3. ^{15}N Relaxation Data for Notch cbEGF11–13.

(A and B) Experimentally determined T_1 and T_2 at (A) 11.7 T and (B) 14.1 T plotted within T_1 and T_2 lines calculated as a function of correlation time, and S^2, using the Lipari-Szabo model (Lipari and Szabo, 1989a, 1989b). In (A) and (B), the points for cbEGF domains 11, 12, and 13 are shown in red, green, and blue, respectively.

(C) [^{1}H]-^{15}N NOE data at 11.7 T (black) and 14.1 T (red).

suggest that N13 is disordered on a slow (μs–ms) timescale, but not on a fast (ps–ns) timescale.

While the relaxation data confirm that the dynamic properties of N13 are different from those of N11–12, they do not inform on the amplitude of domain-domain motions. However, manual analysis of the NOESY data has revealed similar interdomain hydrophobic packing interactions between N11–N12 and N12–N13. Specifically, NOEs have been unambiguously assigned between the structurally equivalent residues Y444–I471 and Y482–I509, which are highlighted in Figure 4A. These data, combined with the relaxation data, support a model in which all three domains are arranged in a linear fashion, with N13 structurally breathing on a slow (μs–ms) timescale. The low density of NOEs for N13 is insufficient to derive a reliable orientation of this domain in the structure calculations; however, one representative structure within the ensemble adopts a linear domain arrangement showing that the NMR data are compatible with this architecture (Figure 4B). Unfortunately, attempts to derive the relative orientation of the domains by using residual dipolar couplings were not successful

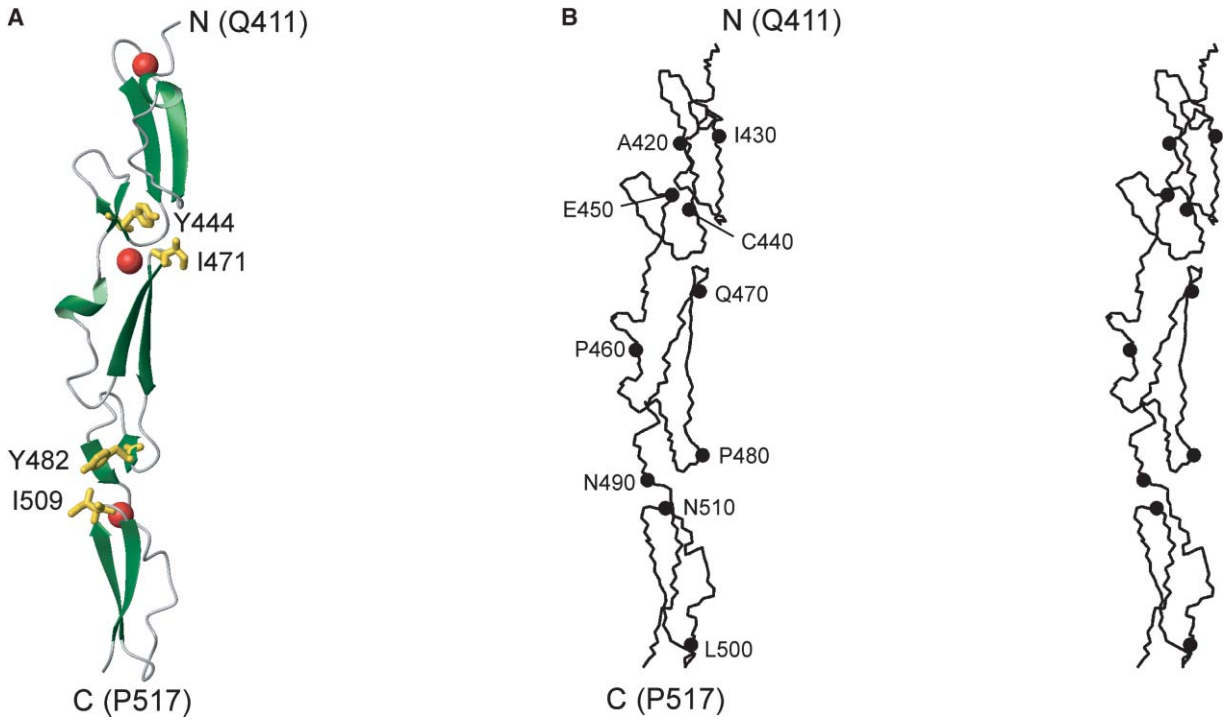

Figure 4. Representative Structure of Notch cbEGF11–13

(A) Schematic ribbon drawing of the representative structure of Notch cbEGF11–13 best fitting the sum of the NMR data. Amino acid residues that pack between adjacent domains, based on the identification of unambiguous long-range NOE crosspeaks, are shown in gold and are labeled. Calcium atoms are depicted as red spheres.

(B) Stereoview (side-by-side) backbone (C^α, C', N) trace of the structure shown in (A) with every tenth C^α atom shown as a sphere and labeled.

due to the problems with line broadening for residues in domain N13 (data not shown). Pairwise domain linkage has been observed previously to affect the structural stability, proteolytic susceptibility, and folding of adjacent domains (Kurniawan et al., 2004; McGettrick et al., 2000; Reinhardt et al., 2000; Werner et al., 2000). Therefore, the increased mobility of N13 is likely to result from the absence of the C-terminally linked EGF14 in this construct.

Discussion

We have expressed and refolded a recombinant fragment containing EGF domains 11–13 of human Notch-1, and we have shown that tetrameric complexes of this peptide bind in a specific and Ca^{2+}-dependent manner to ligand-expressing cells. We thus confirm and extend previous studies, which showed that EGF domains 11 and 12 are responsible for ligand interaction (Rebay et al., 1991), and that Notch binding is dependent upon calcium (Fehon et al., 1990), but not glycosylation of EGF12 (Lei et al., 2003).

Structures were calculated for human Notch-1 EGF domains 11–13 in the presence of saturating calcium at pH 6.1. All three EGF domains adopt a canonical fold that is accurately defined based on criteria for structure calculation convergence, and the orientation of domains 11 and 12 is well defined by the solution NMR data. The combined analysis of NOE and heteronuclear relaxation data reported here indicate that the poor definition of the orientation of domains N12 and N13 in our calculations most likely results from μs–ms timescale motions affecting N13, and not to large-amplitude domain-domain motions. Motions on this timescale have been previously associated with disulphide bond rotamerization in EGF domains (Smallridge et al., 2003; Werner et al., 2000), and it is likely that, in the native Notch molecule, the structure of N13 is stabilized by C-terminal linkage of EGF14.

A schematic illustration of the N11–12 structure is shown in Figure 5 in comparison to the structure of a representative class I pair of cbEGF domains from fibrillin-1 (Downing et al., 1996). It is evident that the two structures show significant similarity in spite of the presence of an extra residue in the linker between the two domains of N11–12. Importantly, however, while the tilt angle for the family of Notch structures, 17° ± 4°, is indistinguishable from to that of previously solved cbEGF pairs (Downing et al., 1996; Saha et al., 2001; Smallridge et al., 2003), the twist angle, 119° ± 5°, is significantly different (Figure 5C).

The axial rotation of one domain with respect to the next is the result of a change in pairwise domain amino acid packing interactions relative to tandem cbEGF domains containing a single amino acid linker. In both cases, there are hydrophobic amino acid interactions involving an aromatic residue in the N-terminal domain; however, in place of the conserved glycine involved in pairwise domain packing in class I pairs, the C-terminal interacting partner of Notch EGF12 is an isoleucine residue (Figure 4). Remarkably, the prediction that the two classes of domain pairs would correspond to two distinct arrangements of EGF domains (Downing et al., 1996) is supported by the conservation of amino acids involved in packing. In PROSITE pattern-based searches of the Swiss-Prot database, 77% of class II EGF-cbEGF or tandem cbEGF pairs contain an aromatic residue (Y/F/W) in the N-terminal domain and a hydrophobic residue (I/L/V/P) in the C-terminal domain at the positions involved in packing (data not shown). These positions are highlighted in Figure 6, which illustrates the consensus sequences for class I and class II EGF-cbEGF/cbEGF-cbEGF domain pairs derived by Downing et al. (Downing et al., 1996). These data strongly suggest that the Notch EGF11–12 structure is a *general* model for many class II EGF domain pairs in which the C-terminal domain is Ca^{2+} saturated, just as the class I consensus sequence-structure relationship has been shown to be general for functionally distinct proteins (Saha et al., 2001). Human proteins containing class II cbEGF domain pairs and a brief description of their functions are given in Table 2. It is of interest to note that all of the proteins apart from Protein S, which contains only a single class II EGF-cbEGF pair, have been proposed to fulfill developmental functions. However, the specific role(s) of the EGF domains within these proteins is in general not well understood.

On the basis of this structure and the amino acid conservation of residues involved in pairwise domain packing of the Notch cbEGFs, we have constructed a model for all 36 EGF domains of the Notch extracellular domain, which is shown in Figure 7. This model shows the domains in the most extended possible conformation; regions containing noncalcium binding EGFs (highlighted) are likely to adopt a less extended interdomain packing arrangement than the tandem cbEGF regions. (In the structure of a pair of noncalcium binding EGF domains from *Plasmodium falciparum* merozoite surface protein-1 (Morgan et al., 1999), the two domains adopt a U-shaped fold, with a large hydrophobic interface, and the current model does not rule out an accordion conformation for the noncalcium binding regions of the extracellular domain.) Nonetheless, the model offers interesting predictions regarding the overall conformation of the Notch receptor, which is expected to be generally elongated in the presence of saturating calcium. In particular, the Notch ligand binding region is contained near the N terminus of the longest stretch of tandem cbEGFs; calcium binding to this region may be important for extending the extracellular domain away from the cell surface and for positioning of the binding site.

Critical to the accuracy of this model is the degree to which Notch cbEGFs are saturated with calcium in the physiological range. The calcium dissociation constant for the C-terminal cbEGF domain of a tandem pair is typically in the micromolar range (Boswell et al., 2004), as was an earlier estimate for Notch EGF12 (Rand et al., 1997). This implies minimal vacancy of Ca^{2+} binding sites at typical extracellular concentrations of around 1 mM. However, a recent study linked unexpectedly large, local fluctuations in extracellular calcium concentration with the regulation of Notch-dependent gene expression in a developmental context (Raya et al., 2004). In a reporter assay, enhanced Delta-dependent Notch signal-

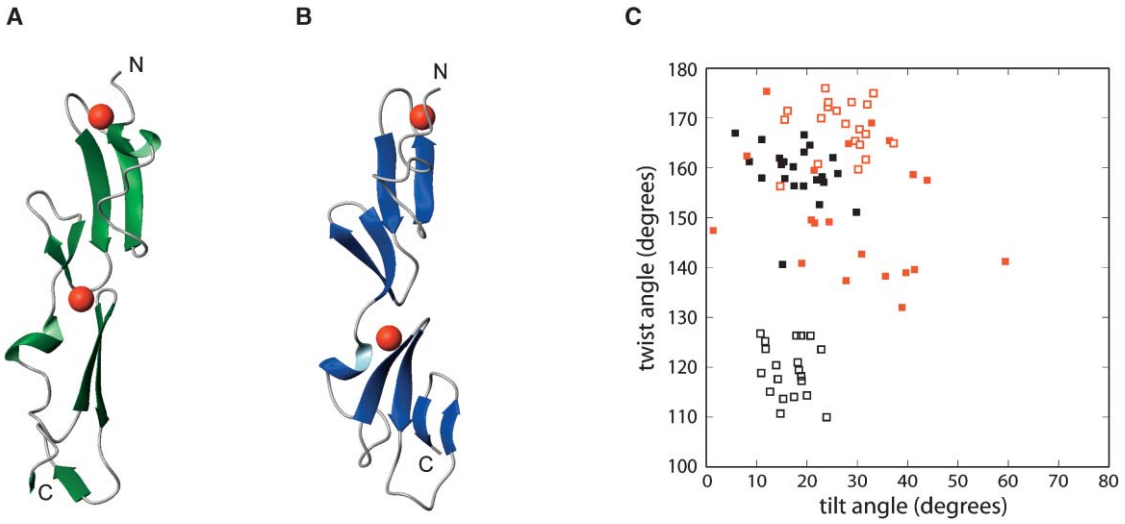

Figure 5. Comparison of Notch cbEGF11–12 Domain Pair Orientation with Class I cbEGF Pairs

(A and B) (A) The tertiary structure of N11–12, a class II cbEGF pair, is shown beside that of (B), an example class I pair (human fibrillin-1 cbEGFs 32 and 33 (Downing et al., 1996)). Notch cbEGF13 is omitted for clarity. The N-terminal EGF domains for the two peptides have been overlaid based on the calcium binding EGF core residues, which are also used for the definition of the tilt and twist angles between the two domains (Downing et al., 1996), and then linearly translated. Note the similar interdomain tilt, but contrasting degrees of twist, resulting in a pair of β strands appearing to flow between the two domains of N11–12.

(C) Angle of twist plotted against angle of tilt for published families of NMR solution structures of cbEGF domain pairs including N11–12 (a class II cbEGF domain pair, black open squares) and class I pairs: fibrillin cbEGFs 32–33 (black filled squares) (Downing et al., 1996), fibrillin cbEGFs 12–13 (red filled squares) (Smallridge et al., 2003), and the LDLR EGF-AB pair (red open squares) (Saha et al., 2001).

ing was shown as the extracellular Ca^{2+} concentration was increased from 0.18 through >5 mM. Although this might be consistent with an effect through increasing Notch cbEGF Ca^{2+} saturation, this cannot be assumed; indeed, the lack of Ca^{2+} sensitivity of Serrate-mediated signaling suggests an effect on Delta rather than Notch.

Since our recombinant protein was expressed in bacteria, the calculated structure lacks posttranslational modifications, including O-linked fucosylation. However, the position of Thr466, upon an exposed surface at the base of the major β hairpin of EGF12 as illustrated in Figure 7, offers insight into the possible role of O-linked oligosaccharide. This position would be expected to be solvent accessible and suggests the possibility of steric interference by O-fucose-linked oligosaccharide as the mechanism of inhibition of Notch signaling by Fringe.

In conclusion, we have described the solution NMR structural and dynamic properties of a refolded, recombinant human Notch-1 peptide that encompasses the ligand binding region. Tetrameric complexes of this peptide display calcium-dependent ligand binding, which suggests that the calcium-dependent behavior of endogenous Notch derives at least in part from calcium binding to this region. NMR analysis of N11–13 has offered a structural correlate of this functional requirement for Ca^{2+}, which participates in a rigid, extended conformation. In addition, we demonstrate a unique interdomain hydrophobic packing arrangement which, based on amino acid conservation, is expected to be prototypi-

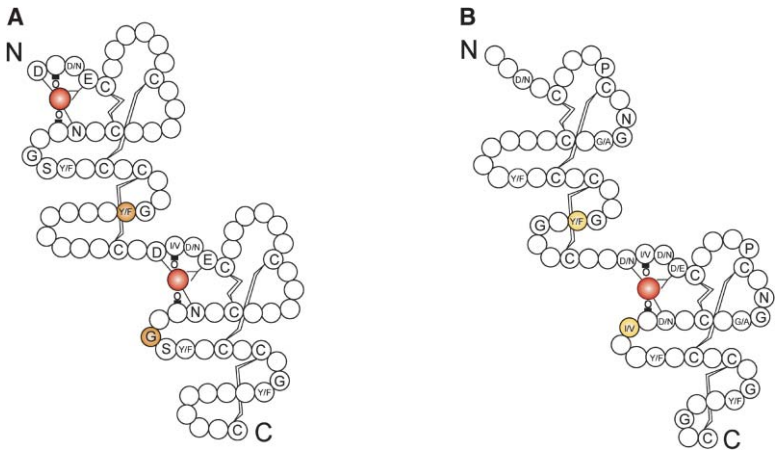

Figure 6. Class I and Class II Consensus Sequences

(A and B) Schematic secondary structure illustrations of (A) class I and (B) class II consensus sequences of EGF-cbEGF/cbEGF-cbEGF domain pairs derived by Downing et al. (Downing et al., 1996). Amino acid residues involved in key pairwise domain hydrophobic packing interactions based on known structures are highlighted in orange and yellow, respectively. Calcium atoms are shaded in red, and potential amino acid side chain and backbone ligands are indicated. Consensus disulphide bonds are illustrated with zigzag connectors.

Table 2. Mammalian Proteins Containing Class II EGF-cbEGF/cbEGF-cbEGF Domain Pairs and Putative Functions Thereof

Protein	Putative Function
Crumbs protein homolog 1	Role in development and maintenance of retinal photoreceptors; mutations produce blinding disorders (Jacobson et al., 2003; Mehalow et al., 2003).
Delta-like protein 1	Ligand for Notch receptors. Involved in development and patterning of a wide variety of tissues (Lai, 2004).
Jagged 1,2	Ligands for multiple Notch receptors. Involved in the mediation of Notch signaling (Lai, 2004). Haploinsufficiency of Jagged 1 produces Alagille syndrome (Harper et al., 2003).
NELL protein 1,2	Modulate calvarial osteoblast differentiation and apoptosis pathways; overexpressed in some forms of craniosynostosis (Zhang et al., 2003).
Notch 1,2,3,4	Receptors for membrane bound ligands of Jagged and Delta-like families; regulating cell-fate determination (Lai, 2004).
Protein S	Anticoagulant plasma protein; a cofactor to activated protein C in the degradation of coagulation factors Va and VIIIa (Esmon, 2000).
Slit 1,2,3	Secreted ligands of Robo in nervous tissue; important for axonal guidance, branching, and neuronal migration (Brose and Tessier-Lavigne, 2000).

Only proteins containing an aromatic residue (Y/F/W) in the N-terminal domain and a hydrophobic residue (I/L/V/P) in the C-terminal domain at the consensus positions involved in class II domain pair packing are listed.

cal of class II cbEGF domains. This insight has enabled modeling of the structure and flexible properties of the majority of the extracellular region of the Notch-1 receptor; it is also likely to be relevant to several other proteins involved in development and other processes.

Experimental Procedures

Expression and Refolding of Recombinant Notch Proteins

The preparation of human Notch-1 cbEGFs 11–13 for structural determination has been described (Muranyi et al., 2004). For the production of tetrameric complexes of Notch, the construct was reengineered to include a 15 amino acid residue BirA recognition sequence at the C terminus (O'Callaghan et al., 1999; Schatz, 1993). Notch cbEGFs 11–13 were reamplified by PCR with *Pfu* polymerase (Stratagene), the template TAN-1 cDNA (Ellisen et al., 1991, a kind gift of Jeffrey Sklar), and primers 5′-TAGTAGGGATCCATAGAAG GACGATCAGCACAGGACGTGGATGAGTGCTCGC-3′ and 5′-TAG TAGAAGCTTGTCGACCTGGCACAGATGCCCAGTGAAGC-3′. Purified PCR product was ligated into the BamHI and Sal1 sites of the bacterial expression vector pQE30 (Qiagen) and cloned in NM554 *E. coli*. The BirA recognition sequence, itself amplified by PCR (from a pGMT7 derivative kindly donated by Dr. C. O'Callaghan), was cloned into the Sal1 site with the introduction of two linker residues. The sequence of the resulting plasmid was confirmed by automated DNA sequencing (ABIprism) and by mass spectrometry of polypeptide product. We detected the same departure from the published sequence as previously described (Rand et al., 1997), resulting in the substitution of methionine with isoleucine at position 477. We confirmed that this was the correct sequence by recloning from an alternative cDNA source, namely, Jurkat cell cDNA. Isoleucine is conserved at this position in Notch-1 of most other species. Expression and refolding was carried out essentially as described (Knott et al., 1996; Muranyi et al., 2004).

Biotinylation and Streptavidin Conjugation

Purified, refolded Notch polypeptide bearing the BirA recognition site was biotinylated overnight at room temperature, by using BirA (Avidity) and the following reaction conditions: 80 mM NaCl, 50 mM Tris-HCl (pH 8), 20 mM $MgCl_2$, 1 mM biotin, and 5 mM ATP (pH 8). The resulting material was acidified and purified by reverse phase HPLC, yielding a single peak that was collected and lyophilized. The efficiency of biotinylation was estimated by the extent of protein adsorption onto streptavidin-agarose beads (Sigma). Known

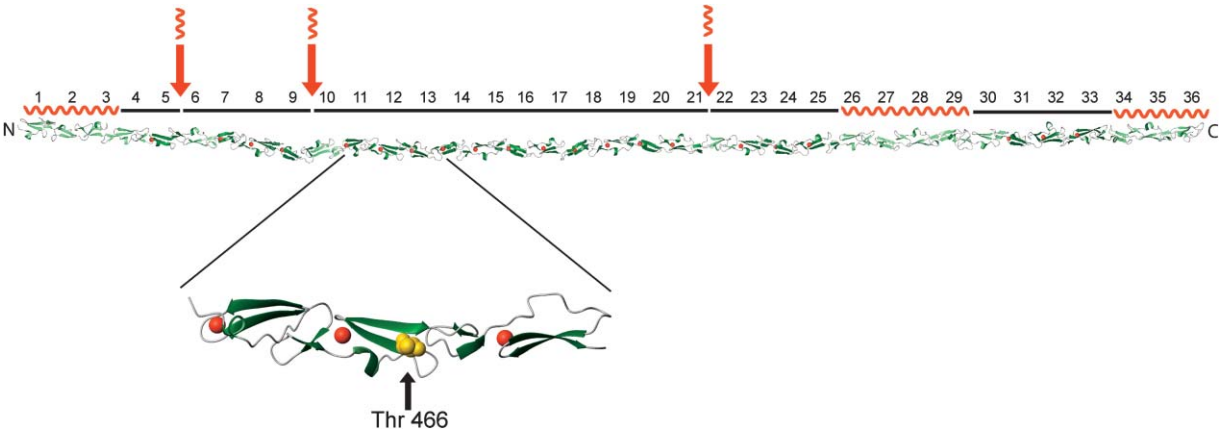

Figure 7. Model of the 36 Notch Extracellular EGF Domains Highlighting the Position of the O-Fucosylation Site

Homology model of the 36 EGF domains of the Notch ECD, color-coded according to putative calcium binding properties (calcium binding, dark green; noncalcium binding, light green). Calcium atoms are shown as red spheres. Solid black lines are drawn over the structure to indicate regions that are predicted to be rigidified when calcium is bound. Red arrows and wavy lines show points and regions of potential flexibility. The experimentally determined structure of EGF11–13 is detailed, highlighting in EGF12 the position of the O-fucosylation site, Thr466, in gold CPK.

amounts of biotinylated sample solution and beads were incubated, with rotation, at 4°C for 30 min. Protein adsorption was measured by the reduction in optical density at 280 nm; after allowing for dilution, this was generally 50%–60%. Tetrameric complexes of recombinant, refolded N11–13 were prepared by mixing the biotinylated monomer with Extravidin-R-phycoerythrin (Extravidin-PE, Sigma) in a 4:1 molar ratio. This was achieved by adding the Extravidin-PE in approximately ten aliquots at intervals of 15–30 min on ice.

FACS Analysis of Notch Tetramer Binding by Ligand-Expressing Cell Lines

L cells expressing murine Delta-like-1 were a kind gift of Professor Maggie Dallman. Ligand expression was driven from a retroviral vector (Wong et al., 2003) and maintained by puromycin selection; proportions of cells stained were in keeping with the efficiency of retroviral transduction. For staining, L cells were detached by brief incubation with 2 mM EDTA in PBS, and cells were washed in cold FACS buffer (150 mM NaCl, 10 mM Tris-HCl [pH 8], 1% fetal calf serum plus 1 mM $CaCl_2$, except where indicated). Cells were incubated for 30–60 min on ice with prediluted Notch tetrameric complexes (1–10 μM) and were washed extensively with FACS buffer prior to fixation (in PBS containing 1% formaldehyde and 1% FCS). As negative controls, tetramer staining was compared with unconjugated Extravidin-PE, and ligand-expressing cells were compared with uninfected L cells (which do not express Notch ligands). Samples were analyzed with FACScan or FACScalibur machines (Becton Dickinson) and CellQuest software.

Solution NMR Data Acquisition and Analysis

Three-dimensional NOESY spectra used for the derivation of distance constraints were acquired as described previously (Muranyi et al., 2004). ^{15}N-edited and ^{13}C-edited NOESY spectra were measured with mixing times of 150 ms and 100 ms, respectively. A series of HSQC (Kay, 1992 #2) spectra recorded directly after dissolving the sample in ^2H_2O were used to identify slowly exchanging amide ^1H as peaks present after 24 hr. The NMR data were processed with Felix 97 (MSI, Inc.).

NMRView, version 5.0.4 (Johnson and Blevins, 1994), was used to facilitate NOE assignment. The previously reported chemical shifts for $^1H\alpha$, $^{13}C\alpha$, $^{13}C\beta$, and $^{13}C'$ (Muranyi et al., 2004) were analyzed with TALOS (Cornilescu et al., 1999) to derive backbone dihedral angle restraints. Slowly exchanging amide protons identified in well-defined regions of β sheet or α-helical secondary structures were subjected to two hydrogen bond distance constraints, $d_{O\text{-}N} = 3.0 \pm 0.3$ Å and $d_{O\text{-}HN} = 2.0 \pm 0.3$ Å.

Relaxation data of calcium-saturated N11–13 were acquired at 25°C on home-built/GE Omega spectrometers operating at 500 and 600 MHz as described previously (Werner et al., 2001). Each spectrometer was fitted with a triple resonance probe with self-shielded pulsed field gradients. In the ^{15}N-T_1 and ^{15}N-T_2 experiments (Farrow et al., 1994), the acquisition times were 151 ms (^1H) and 52.2 ms (^{15}N) at 500 MHz and 128 ms (^1H) and 43.5 ms (^{15}N) at 600 MHz. The CPMG delay in the T_2 experiment was set to 500 μs. Relaxation delays were 40, 80, 120, 160, 240, 400, 800, and 1200 ms and 8, 16, 24, 32, 40, 64, 80, and 120 ms for the T_1 and the T_2 series, respectively. T_1 and T_2 relaxation time constants were derived from two-parameter exponential fits to the intensity decays, and errors were estimated from the root mean square noise in the spectra.

Pairs of 2D ^1H-detected [^1H]-^{15}N heteronuclear NOE experiments (Farrow et al., 1994) were acquired at 500 and 600 MHz at a temperature of 25°C with acquisition times of 128 ms (^1H) and 32.6 ms (^{15}N). ^1H saturation was achieved in the experiment with NOE by a train of 120° flip angle ^1H pulses at 5 ms intervals for 3 s. The [^1H]-^{15}N NOE was calculated as the ratio of the peak volumes in the experiments with and without proton saturation. The relaxation data were also analyzed with NMRView (Johnson and Blevins, 1994).

Automated Solution NMR Structure Calculations with CYANA

The NMRView sequence, chemical shift, and cross peak files were converted to XEASY format by using the CCPN format converter v1.0b11 (Wranken, 2004). The intensities of 1,894 peaks and 2,219 peaks picked in the ^{15}N- and ^{13}C-edited NOESY spectra, respectively, and the previously reported chemical shifts were used as input for structure calculations with CYANA software and the CANDID protocol (Herrmann et al., 2002). Additional restraints included 44 ϕ and 43 ψ dihedral angle restraints, 42 distance restraints for 21 hydrogen bonds, 15 distance restraints for calcium ligation, incorporated as described previously (Downing et al., 1996), and 9 disulphide bonds according to the known pattern associated with EGF domains (Boswell et al., 2004). Three calcium atoms were incorporated based on the high-resolution crystal structure of a cbEGF domain (Rao et al., 1995). This was achieved by the modification of the CYANA library file to include modified amino acids with a calcium atom attached covalently to the oxygen of the C′=O ligand at a linear distance of 2.28 Å in position x of the N-terminal region of the calcium binding consensus sequence D/N-x-D/N-E, corresponding to residues V^{413}, V^{453}, and T^{491}.

Chemical shift degeneracy of the ^{13}C-edited NOESY spectrum led to poor structural convergence and a compacted multidomain structure that was not consistent with manual inspection of the NOESY data. Therefore, an initial structure was calculated on the basis of the ^{15}N-edited NOESY data alone and was used as a template for final structure calculations utilizing the complete set of experimental data. Typically, 600 conformers were calculated, and the 20 best were selected for each assignment cycle. An iterative structure refinement was performed within cycle 7 in which the assignments of violated or unassigned peaks were adjusted manually. Twenty final structures were selected based upon the convergence criteria described by Jee and Güntert (Jee and Güntert, 2003). Structural statistics and measures of convergence for the ensemble are given in Table 1. Tilt and twist angles for the two domains of N11–12 were calculated by using previously described methods (Downing et al., 1996).

Amino Acid Sequence Analysis and Homology Modeling Methods

In order to identify class II EGF-cbEGF and tandem cbEGF pairs with or without consensus residues involved in pairwise domain packing, ScanProsite (Gattiker et al., 2002) was run on the Swiss-Prot Release 43.5 release (Boeckmann et al., 2003) with the templates X(4)-C-{C}(2,14)-C-{C}(2,8)-C-{C}(2,12)-C-{C}-C-{C}(2,20)-C-{C}(2)-[QDNE]-{C}-[QDNE]-[QDNE]-C-{C}(2,14)-C-{C}(2,8)-C-{C}-[QDNE]-{C}(2,8)-[YF]-{C}-C-{C}-C-{C}(2,20)-C and X(4)-C-{C}(2,14)-C-{C}(2,8)-C-{C}(2,12)-C-{C}-C-{C}(2,6)-[YFW]-{C}(2,20)-C-{C}(2)-[QDNE]-{C}-[QDNE]-[QDNE]-C-{C}(2,14)-C-{C}(2,8)-C-{C}-[QDNE]-{C}-[IVLP]-{C}(2,6)-[YF]-{C}-C-{C}-C-{C}(2,20)-C, respectively, and excluding splice variants. Sequences were aligned with Clustal-X (Thompson et al., 1997) with default parameters and were adjusted by using profile alignment methods to correct the alignment of EGF consensus cysteine residues. Homology modeling of the 36 EGF domains of the Notch extracellular domain was performed with Modeller 6v2 (Fiser and Sali, 2003) by using the representative structure of N11–13 shown in Figure 4 as a template. Calcium atoms were incorporated into the model, and Powell energy minimization was performed with CNS 1.1 (Brunger et al., 1998).

Acknowledgments

S.H. and A.J.M. were supported by the Medical Research Council. A.K.D. is a Wellcome Trust Senior Research Fellow (057725). N.V.V. is a Wellcome Trust Prize Student (070417). V.K. and P.A.H. were supported by the MRC (Grant No. G000164). A.M. was supported by a postdoctoral grant from the Wenner-Gren Foundations.

Received: August 19, 2004
Revised: September 21, 2004
Accepted: September 21, 2004
Published: December 7, 2004

References

Altman, J.D., Moss, P.A., Goulder, P.J., Barouch, D.H., McHeyzer-Williams, M.G., Bell, J.I., McMichael, A.J., and Davis, M.M. (1996).

Phenotypic analysis of antigen-specific T lymphocytes. Science *274*, 94–96.

Boeckmann, B., Bairoch, A., Apweiler, R., Blatter, M.-C., Estreicher, A., Gasteiger, E., Martin, M.J., Michoud, K., O'Donovan, C., Phan, I., et al. (2003). The SWISS-PROT protein knowledgebase and its supplement TrEMBL in 2003. Nucleic Acids Res. *31*, 365–370.

Boswell, E., Kurniawan, N., and Downing, A.K. (2004). Calcium binding EGF-like domains. In Handbook of Metalloproteins, Volume 3, A. Messerschmidt, ed. (New York: Wiley), pp. 553–570.

Brose, K., and Tessier-Lavigne, M. (2000). Slit proteins: key regulators of axon guidance, axonal branching, and cell migration. Curr. Opin. Neurobiol. *10*, 95–102.

Brunger, A.T., Adams, P.D., Clore, G.M., DeLano, W.L., Gros, P., Grosse-Kunstleve, R.W., Jiang, J.S., Kuszewski, J., Nilges, M., Pannu, N.S., et al. (1998). Crystallography & NMR system: a new software suite for macromolecular structure determination. Acta Crystallogr. D Biol. Crystallogr. *54*, 905–921.

Cardy, C.M., and Handford, P.A. (1998). Metal ion dependency of microfibrils supports a rod-like conformation for fibrillin-1 calcium-binding epidermal growth factor-like domains. J. Mol. Biol. *276*, 855–860.

Cornilescu, G., Delaglio, F., and Bax, A. (1999). Protein backbone angle restraints from searching a database for chemical shift and sequence homology. J. Biomol. NMR *13*, 289–302.

de Celis, J.F., Barrio, R., Delarco, A., and Garciabellido, A. (1993). Genetic and molecular characterization of a Notch mutation in its Delta-binding and Serrate-binding domain in *Drosophila*. Proc. Natl. Acad. Sci. USA *90*, 4037–4041.

Downing, A.K., Knott, V., Werner, J.M., Cardy, C.M., and Campbell, I.D. (1996). Solution structure of a pair of calcium binding epidermal growth factor-like domains: implications for the Marfan syndrome and other genetic disorders. Cell *85*, 597–605.

Ellisen, L.W., Bird, J., West, D.C., Soreng, A.L., Reynolds, T.C., Smith, S.D., and Sklar, J. (1991). Tan-1, the human homolog of the *Drosophila* Notch gene, is broken by chromosomal translocations in T-lymphoblastic neoplasms. Cell *66*, 649–661.

Esmon, C.T. (2000). Regulation of blood coagulation. Biochim. Biophys. Acta *1477*, 349–360.

Farrow, N.A., Zhang, O.W., Forman-Kay, J.D., and Kay, L.E. (1994). A heteronuclear correlation experiment for simultaneous determination of N-15 longitudinal decay and chemical-exchange rates of systems in slow equilibrium. J. Biomol. NMR *4*, 727–734.

Fehon, R.G., Kooh, P.J., Rebay, I., Regan, C.L., Xu, T., Muskavitch, M.A.T., and Artavanis-Tsakonas, S. (1990). Molecular-interactions between the protein products of the neurogenic loci Notch and Delta, 2 EGF-homologous genes in *Drosophila*. Cell *61*, 523–534.

Fiser, A.S., and Sali, A. (2003). MODELLER: generation and refinement of homology-based protein structure models. Methods Enzymol. *374*, 461–491.

Garces, C., Ruiz-Hidalgo, M.J., de Mora, J.F., Park, C., Miele, L., Goldstein, J., Bonvini, E., Porras, A., and Laborda, J. (1997). Notch-1 controls the expression of fatty acid-activated transcription factors and is required for adipogenesis. J. Biol. Chem. *272*, 29729–29734.

Gattiker, A., Gasteiger, E., and Bairoch, A. (2002). ScanProsite: a reference implementation of a PROSITE scanning tool. Appl. Bioinformatics *1*, 107–108.

Han, W., Ye, Q., and Moore, M.A.S. (2000). A soluble form of human Delta-like-1 inhibits differentiation of hematopoietic progenitor cells. Blood *95*, 1616–1625.

Harper, J.A., Yuan, J.S., Tan, J.B., Visan, I., and Guidos, C.J. (2003). Notch signaling in development and disease. Clin. Genet. *64*, 461–472.

Henderson, S.T., Gao, D., Christensen, S., and Kimble, J. (1997). Functional domains of LAG-2, a putative signaling ligand for LIN-12 and GLP-1 receptors in *Caenorhabditis elegans*. Mol. Biol. Cell *8*, 1751–1762.

Herrmann, T., Güntert, P., and Wüthrich, K. (2002). Protein NMR structure determination with automated NOE assignment using the new software CANDID and the torsion angle dynamics algorithm DYANA. J. Mol. Biol. *319*, 209–227.

Jacobson, S.G., Cideciyan, A.V., Aleman, T.S., Pianta, M.J., Sumaroka, A., Schwartz, S.B., Smilko, E.E., Milam, A.H., Sheffield, V.C., and Stone, E.M. (2003). Crumbs homolog 1 (CRB1) mutations result in a thick human retina with abnormal lamination. Hum. Mol. Genet. *12*, 1073–1078.

Jee, J.G., and Güntert, P. (2003). Influence of the completeness of chemical shift assignments on NMR structures obtained with automated NOE assignment. J. Struct. Funct. Genomics *4*, 179–189.

Johnson, B.A., and Blevins, R.A. (1994). NMRView—a computer program for the visualization and analysis of NMR data. J. Biomol. NMR *4*, 603–614.

Kielty, C.M., and Shuttleworth, C.A. (1993). The role of calcium in the organization of fibrillin microfibrils. FEBS Lett. *336*, 323–326.

Knott, V., Downing, A.K., Cardy, C.M., and Handford, P. (1996). Calcium binding properties of an epidermal growth factor-like domain pair from human fibrillin-1. J. Mol. Biol. *255*, 22–27.

Koradi, R., Billeter, M., and Wüthrich, K. (1996). MOLMOL: a program for display and analysis of macromolecular structures. J. Mol. Graph. *14*, 51–55.

Kurniawan, N., O'Leary, J., Thamlitz, A.-M., Sofair, R., Werner, J.M., Stenflo, J., and Downing, A.K. (2004). N-terminal domain linkage modulates the folding properties of protein S EGF modules. Biochemistry *43*, 9352–9360.

Lai, E.C. (2004). Notch signaling: control of cell communication and cell fate. Development *131*, 965–973.

Lawrence, N., Klein, T., Brennan, K., and Arias, A.M. (2000). Structural requirements for Notch signalling with Delta and Serrate during the development and patterning of the wing disc of *Drosophila*. Development *127*, 3185–3195.

Lei, L., Xu, A.G., Panin, V.M., and Irvine, K.D. (2003). An O-fucose site in the ligand binding domain inhibits Notch activation. Development *130*, 6411–6421.

Lipari, G., and Szabo, A. (1989a). Model-free approach to the interpretation of nuclear magnetic resonance relaxation in macromolecules. 1. Theory and range of validity. J. Am. Chem. Soc. *104*, 4546–4559.

Lipari, G., and Szabo, A. (1989b). Model-free approach to the interpretation of nuclear magnetic resonance relaxation in macromolecules. 2. Analysis of experimental results. J. Am. Chem. Soc. *104*, 4559–4570.

McGettrick, A.J., Knott, V., Willis, A., and Handford, P.A. (2000). Molecular effects of calcium binding mutations in Marfan syndrome depend on domain context. Hum. Mol. Genet. *9*, 1987–1994.

Mehalow, A.K., Kameya, S., Smith, R.S., Hawes, N.L., Denegre, J.M., Young, J.A., Bechtold, L., Haider, N.B., Tepass, U., Heckenlively, J.R., et al. (2003). CRB1 is essential for external limiting membrane integrity and photoreceptor morphogenesis in the mammalian retina. Hum. Mol. Genet. *12*, 2179–2189.

Moloney, D.J., Panin, V.M., Johnston, S.H., Chen, J., Shao, L., Wilson, R., Wang, Y., Stanley, P., Irvine, K.D., Haltiwanger, R.S., et al. (2000). Fringe is a glycosyltransferase that modifies Notch. Nature *406*, 369–375.

Morgan, W.D., Birdsall, B., Frenkiel, T.A., Gradwell, M.G., Burghaus, P.A., Syed, S.E.H., Uthaipibull, C., Holder, A.A., and Feeney, J. (1999). Solution structure of an EGF module pair from the plasmodium falciparum merozite surface protein 1. J. Mol. Biol. *289*, 113–122.

Muranyi, A., Hambleton, S., Knott, V., McMichael, A., Handford, P.A., and Downing, A.K. (2004). Letter to the Editor: ^{1}H, ^{13}C, and ^{15}N resonance assignments of human Notch-1 calcium binding EGF domains 11–13. J. Biomol. NMR *3*, 443–444.

Nickoloff, B.J., Qin, J.Z., Chaturvedi, V., Denning, M.F., Bonish, B., and Miele, L. (2002). Jagged-1 mediated activation of notch signaling induces complete maturation of human keratinocytes through NF-kappaB and PPARgamma. Cell Death Differ. *9*, 842–855.

O'Callaghan, C.A., Byford, M.F., Wyer, J.R., Willcox, B.E., Jakobsen, B.K., McMichael, A.J., and Bell, J.I. (1999). BirA enzyme: production

and application in the study of membrane receptor-ligand interactions by site-specific biotinylation. Anal. Biochem. *266*, 9–15.

Okajima, T., and Irvine, K.D. (2002). Regulation of notch signaling by O-linked fucose. Cell *111*, 893–904.

Okajima, T., Xu, A., and Irvine, K.D. (2003). Modulation of Notch-ligand binding by protein O-fucosyltransferase 1 and Fringe. J. Biol. Chem. *278*, 42340–42345.

Rand, M.D., Lindblom, A., Carlson, J., Villoutreix, B.O., and Stenflo, J. (1997). Calcium binding to tandem repeats of EGF-like modules. Expression and characterization of the EGF-like modules of human Notch-1 implicated in receptor-ligand interactions. Protein Sci. *6*, 2059–2071.

Rao, Z., Handford, P., Mayhew, M., Knott, V., Brownlee, G.G., and Stuart, D. (1995). The structure of a Ca^{2+}-binding epidermal growth factor-like domain: its role in protein-protein interactions. Cell *82*, 131–141.

Raya, A., Kawakami, Y., Rodriguez-Esteban, C., Ibanes, M., Rasskin-Gutman, D., Rodriguez-Leon, J., Buscher, D., Feijo, J., and Belmonte, J.C.I. (2004). Notch activity acts as a sensor for extracellular calcium during vertebrate left-right determination. Nature *427*, 121–128.

Rebay, I., Fleming, R.J., Fehon, R.G., Cherbas, L., Cherbas, P., and Artavanis-Tsakonas, S. (1991). Specific EGF repeats of Notch mediate interactions with Delta and Serrate: implications for Notch as a multifunctional receptor. Cell *67*, 687–699.

Reinhardt, D.P., Ono, R.N., Notbohm, H., Muller, P.K., Bachinger, H.P., and Sakai, L.Y. (2000). Mutations in calcium-binding epidermal growth factor modules render fibrillin-1 susceptible to proteolysis - a potential disease-causing mechanism in Marfan syndrome. J. Biol. Chem. *275*, 12339–12345.

Saha, S., Boyd, J., Werner, J.M., Knott, V., Handford, P.A., Campbell, I.D., and Downing, A.K. (2001). Solution structure of the LDL receptor EGF-AB pair: a paradigm for the assembly of tandem calcium binding EGF domains. Structure *9*, 451–456.

Schatz, P.J. (1993). Use of peptide libraries to map the substrate-specificity of a peptide-modifying enzyme - a 13 residue consensus peptide specifies biotinylation in *Escherichia coli*. Biotechnology *11*, 1138–1143.

Schweisguth, F. (2004). Regulation of Notch signaling activity. Curr. Biol. *14*, R129–R138.

Shao, L., Moloney, D.J., and Haltiwanger, R. (2003). Fringe modifies O-fucose on mouse Notch1 at epidermal growth factor-like repeats within the ligand-binding site and the abruptex region. J. Biol. Chem. *278*, 7775–7782.

Shimizu, K., Chiba, S., Kumano, K., Hosoya, N., Takahashi, T., Kanda, Y., Hamada, Y., Yazaki, Y., and Hirai, H. (1999). Mouse Jagged1 physically interacts with Notch2 and other Notch receptors - assessment by quantitative methods. J. Biol. Chem. *274*, 32961–32969.

Smallridge, R.S., Whiteman, P., Werner, J.M., Campbell, I.D., Handford, P.A., and Downing, A.K. (2003). Solution structure and dynamics of a calcium binding epidermal growth factor-like domain pair from the neonatal region of human fibrillin-1. J. Biol. Chem. *278*, 12199–12206.

Thompson, J.D., Gibson, T.J., Plewniak, F., Jeanmougin, F., and Higgins, D.G. (1997). The CLUSTAL_X windows interface: flexible strategies for multiple sequence alignment aided by quality analysis tools. Nucleic Acids Res. *25*, 4876–4882.

Werner, J.M., Knott, V., Handford, P.A., Campbell, I.D., and Downing, A.K. (2000). Backbone dynamics of a cbEGF domain pair in the presence of calcium. J. Mol. Biol. *296*, 1065–1078.

Werner, J.M., Campbell, I.D., and Downing, A.K. (2001). Shape and dynamics of a calcium binding EGF domain pair investigated by ^{15}N-NMR relaxation. Methods Mol. Biol. *173*, 285–300.

Whiteman, P., Smallridge, R.S., Knott, V., Cordle, J.J., Downing, A.K., and Handford, P.A. (2001). A G1127S change in calcium-binding epidermal growth factor-like domain 13 of human fibrillin-1 causes short range conformational effects. J. Biol. Chem. *276*, 17156–17162.

Wong, K.K., Carpenter, M.J., Young, L.L., Walker, S.J., McKenzie, G., Rust, A.J., Ward, G., Packwood, L., Wahl, K., Delriviere, L., et al. (2003). Notch ligation by Delta1 inhibits peripheral immune responses to transplantation antigens by a CD8+ cell-dependent mechanism. J. Clin. Invest. *112*, 1741–1750.

Wranken, W. (2004). FormatConverter v1.0b11 (http://www.ccpn.ac.uk).

Zhang, X., Carpenter, D., Bokui, N., Soo, C., Miao, S., Truong, T., Wu, B., Chen, I., Vastardis, H., Tanizawa, K., et al. (2003). Overexpression of Nell-1, a craniosynostosis-associated gene, induces apoptosis in osteoblasts during craniofacial development. J. Bone Miner Res. *18*, 2126–2134.

Accession Numbers

N11-13 and the final constraints used in the structure calculations have been deposited in the Protein Data Bank with accession number 1TOZ.